An Experimental Introduction to Optical Pumping And the Zeeman Effect in ^{85}Rb, ^{87}Rb*

Abhishek Cherath
Stony Brook University
(Dated: December 10, 2021)

I offer a brief, mostly qualitative illustrative introduction to the experimental observation of the Zeeman effect in Rubidium using optical pumping. The Zeeman energies thus obtained are used to infer the Earth's magnetic field (at Stony Brook), and the hyperfine Landé g-factors for ^{87}Rb, ^{85}Rb. Further, I report an observation of multiphoton absorptions in optically pumped ^{87}Rb, and a brief theoretical motivation for the same.

I. INTRODUCTION:

A. Brief Introduction to the Zeeman Effect

In an atomic system, the electron experiences a magnetic field due to the field created by the positively charged nucleus, let this field be B_{int}. When $B_{ext} << B_{int}$, the Zeeman perturbation can be modeled as a first order perturbation on top of the fine structure Hamiltonian. This gives the energy correction term:

$$E'_z = \langle nljm_j|H'_z|nljm_j\rangle = \frac{e}{2m}\mathbf{B}_{ext}\cdot\langle\mathbf{L}+\mathbf{2S}\rangle$$

$$\langle\mathbf{L}+\mathbf{2S}\rangle = \left\langle\left(1+\frac{\mathbf{S}\cdot\mathbf{J}}{J^2}\right)\mathbf{J}\right\rangle$$

Where $\mathbf{J}=\mathbf{L}+\mathbf{S}$ is the total angular momentum. Expressing the angular momenta in terms of their quantum numbers gives:

$$E'_z = \mu_B g_F B_{ext} m_F \tag{1}$$

where g_F is the hyperfine Landé g-factor, and μ_B is the Bohr magneton given by $\frac{e\hbar}{2m} = 5.788\times10^{-5}\ eV/T$ So, in the presence of a magnetic field, the Zeeman effect splits energies of the previously degenerate 2F+1 states, where $\mathbf{F}=\mathbf{S}+\mathbf{L}+\mathbf{I}$ where $\mathbf{S},\mathbf{L}$ are the spin and orbital angular momenta of an electron (This analysis is simple in the case of Rubidium as it has only one electron in its valence shell.)

1. *Prediction for Hyperfine Landé g-factor in ^{85}Rb and ^{87}Rb*

The landé g-factor is given by

$$g_J = g_L\frac{J(J+1)-S(S+1)+L(L+1)}{2J(J+1)} + g_S\frac{J(J+1)+S(S+1)-L(L+1)}{2J(J+1)} \tag{2}$$

$g_L = 1$ and $g_S \approx 2$ (ignoring Dirac formula and QCD correction terms.)

$$g_J = 1+\frac{J(J+1)+S(S+1)-L(L+1)}{2J(J+1)}$$

For hyperfine landé factor:

$$g_F \approx g_J\frac{F(F+1)-I(I+1)+J(J+1)}{2F(F+1)} \tag{3}$$

Which gives predicted $g_F = 0.5$ for ^{85}Rb and $g_f = 0.33$ for ^{87}Rb.

B. Apparatus & Mechanism of Optical Pumping

Optical pumping requires spin polarized light at the frequency of some transition for ^{87}Rb,^{85}Rb. Rb atoms have 37 electrons, and a ground state configuration of $1s^22s^22p^63s^23p^63d^{10}4s^24p^65s$. Notably (like other alkali metals) it only has one electron in its outer shell. This makes the spectroscopy quite simple, since the low energy ground state transition is a simple $s-p$ transition (albeit slightly complicated by the fact that there are two possible P energies because of spin-orbit coupling.)

The D_1 spectral line is used in this experiment, supplied by a rubidium discharge lamp (Which obviously emits at the required absorption lines.) A cell with Natural Rubidium (So both ^{85}Rb and ^{87}Rb are present) and nonreactive Argon buffer gas at about 2500 Pa is placed in between this lamp and a photodiode.

The rubidium absorbs the D_1 light when its in gas form. While its boiling point is too high ($688°C$) to achieve reasonably in the lab; it has high vapor pressure, so a good absorption cross section can be achieved at low temperatures of around $30°C$. Now, the rubidium also *emits* D_1 light, but since the light from the lamp is pointed toward the photodiode, and emitted light has no directional preference, a significant decrease in intensity is observed.

Basic selection rules stipulate that for the D_1 transition:

1. $\Delta J = 0$

* With a note on Multiphoton Transitions.

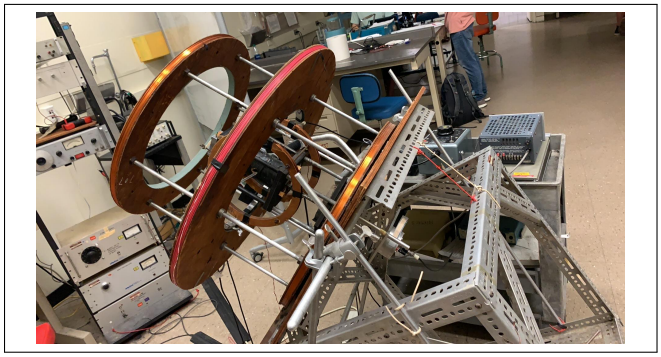

Figure 1. Photograph of Apparatus, Showing Maxwell and Helmholtz coils [6].

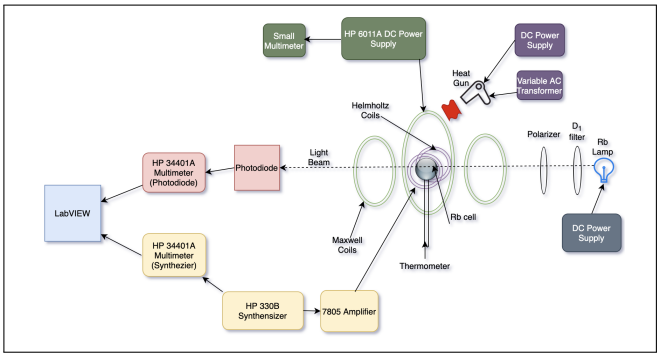

Figure 2. Apparatus Connection Diagram [6].

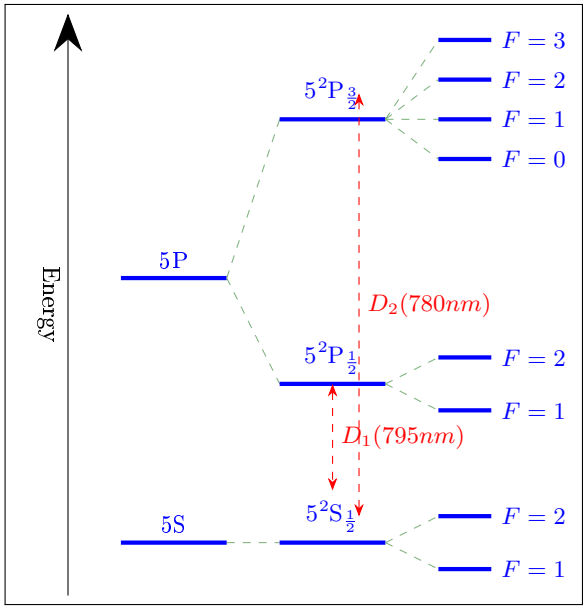

Figure 3. ^{87}Rb energy transitions

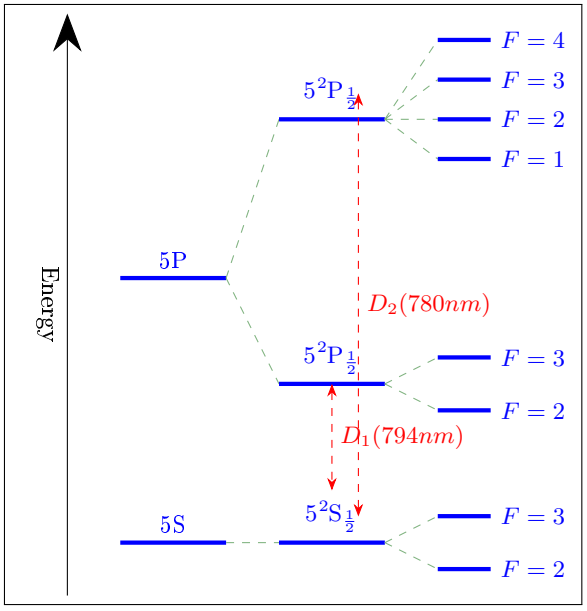

Figure 4. ^{85}Rb energy transitions

2. $\Delta M = 0, \pm 1$

Electrons in the excited $5^2P_{1/2}$ state are unstable, and rapidly undergoes spontaneous emission (in $\approx 30\,ns$) to return to the $5^2S_{1/2}$ state. The three ΔM changes happen with about equal probability in both absorption and emission, so the different magnetic sub levels are equally populated. An atom is considered "pumped" when one of these magnetic sub levels is much likelier to be populated than the others.

To induce pumping, a polarizer + quarter wave-plate filter set is placed in between the rubidium cell and the lamp. This causes all the light entering the cell to be σ_+ or σ_- polarized. The apparatus is tilted to align with Earth's magnetic field to ensure that the direction of propagation is parallel to the magnetic field, as otherwise absorption will be limited. Without loss of generality, assume σ_+. Then, the only allowed transition is $\Delta M = 1$! Therefore, in every absorption-emission event pair, the magnetic quantum number increases on average by 1. But in the $5^2S_{1/2}M_F = 2$ state, the $\Delta M = 1$ transition is no longer permitted, since there is no $5^2P_{1/2}M_F = 3$ state. So, assuming no thermal transitions, eventually all the valence electrons will be in the $5^2S_{1/2}M_F = 2$ state.

The energy difference of the different magnetic sub levels *(Zeeman Splitting)* corresponds to radio waves on the order of $1\,kHz$ with a magnetic field of about $100\,\mu T$. This transition can be stimulated by applying an RF field, which is very easy to achieve with a function generator and a set of Helmholtz coils (with an amplifier to increase the rate of stimulated emission.) The magnetic field can be supplied by the Earth, or by a set of large coils to create a constant magnetic field throughout the cell.

This stimulated emission causes the electrons in the non-absorbing $5^2S_{1/2}M_F = 2$ state to enter the absorbing $5^2S_{1/2}M_F = 1$ state, which reduces light intensity at the photodiode. Sweeping the RF frequency around the sub level resonance shows a characteristic Lorentzian shape due to pressure broadening. The resonant energy

can be compared with the theory value (from the Breit-Rabi formula), which is used to infer the magnetic field of the Earth and the Landé g-factor of the atom under consideration.

C. Qualitative Discussion of the Physics Involved.

In the process of optical pumping, not *all* electrons end up in the pumped state (F=2 for ^{87}Rb.) At room temperature, with 0 magnetic field, a roughly 1% decrease in intensity is observed. If all electrons were in the pumped state, assuming that the only light source is from $\sigma = \pm 1$ light, a much greater drop would be expected when the Zeeman states become degenerate. The observation is explained by temperature, since the kinetic energy imbued during collisions at room temperature is sufficient to move electrons between Zeeman states. So, in the absence of circularly polarized light, all of the Zeeman states are roughly in equilibrium, whereas with the light relatively more electrons are in the extreme m states ($m = \pm 2$ in the case of Rubidium.)[9]

This understanding of the observed intensity reduction at the photodetector also explains observations at high temperatures and the reason behind the varying peak heights in the high B field regime. When a resonant RF field (moving electrons from $m = i$ to $m = i-1$) is applied to the Rubidium gas sample, it changes the equilibrium, and has two effects:

1. *case* $m = 2$: Here, the explanation for increased absorption is simple, electrons exit the non absorbing state and enter absorbing states, reducing photon intensity at the photodetector.

2. *case* $m < 2$: Here, the explanation involves two steps. First the transition opens more space in the from m state of the resonance, moving the thermal equilibrium from the non absorbing $m = 2$ state to an absorbing $m < 2$ state. This also reduces the amount of non absorbing photons, albeit by a lesser amount than in the extreme case, with the effect reducing further from the $m = 2$ state, since the number of electrons reduces further from the extreme m state (This is because due to the pumping effect, electrons reach the further states by multiple thermal transitions from the extreme m state.)

However, when temperature increases, the equilibrium moves in favor of thermal transitions, which simultaneously reduces the absolute magnitude of the intensity reduction at resonance while increasing the relative effect of 2. This may explain the strange "twin peak" behavior seen at high temperatures even with low B fields ($\approx 30\mu T$).

Further, when the applied RF field frequency is the arithmetic mean of subsequent RF resonance frequencies, an increase in photon absorption is expected, since there should be a multiphoton transition between $m = i$ and $m = i - 2$. I attempted to observe this effect, and the result is recorded in Section II D.

II. RESULTS

A. Calculating Landé g-factor from measured pumped absorption spectra

A known magnetic field is applied to the rubidium cell (details in attached notebook.) The virtual photon dip frequency corresponding with the Zeeman energy difference should obey the following relation.

$$hf = \mu_B g_F \boldsymbol{B}_{\text{ext}} \tag{4}$$

The magnetic field $\boldsymbol{B}_{\text{ext}}$ is inferred from the measured value for current in the Maxwell coils, using Equation 5.[10]

$$B = \frac{\mu_0 I}{2} \sum_i \frac{n_i R_i^2}{(R_i^2 + x_i^2)^{3/2}} \tag{5}$$

Plotting the observed RF resonance frequency vs the magnetic field yields the plot in Figure 6 , whose slope should be $\frac{\mu_B g_F}{h}$. From the least squares fit for these points, the inferred Landé g-factors are:

1. $g_f(^{87}Rb) = 0.4915 \pm 0.0005$
2. $g_f(^{85}Rb) = 0.3267 \pm 0.0002$

These values do not quite agree with the theoretical values of 0.5, 0.33 respectively. This could be because of underestimating the error introduced by one or more of our experiment's components. The most likely source is a correction term in Equation 5 because the magnetic field created by the Maxwell coils does not exactly match the idealized prediction. Experimentally measuring the field instead of inferring it would confirm this hypothesis and will be an improvement to the setup.

B. Calculating Earth's Magnetic Field

The y-intercept of the lines in Figure 6 should be given by $f_{\text{intercept}} = \frac{B_{\text{earth}} \mu_B g_j}{h}$. From that, and the g_F values acquired earlier, Earth's magnetic field is predicted to be $44020 \pm 170\, nT$ (from ^{85}Rb intercept) and $43140 \pm 290\, nT$ (from ^{87}Rb intercept.) These values do not agree with the value of $51259.6 \pm 145\, nT$ obtained from NOAA's magnetic field calculation tool [4], but this is not unexpected, since there is a lot of magnetic interference from sources within the physics building.

C. The Quadratic Zeeman and Paschen-Back Effect

In the high magnetic field regime, the Zeeman effect is also called the Paschen-Back effect. What happens here

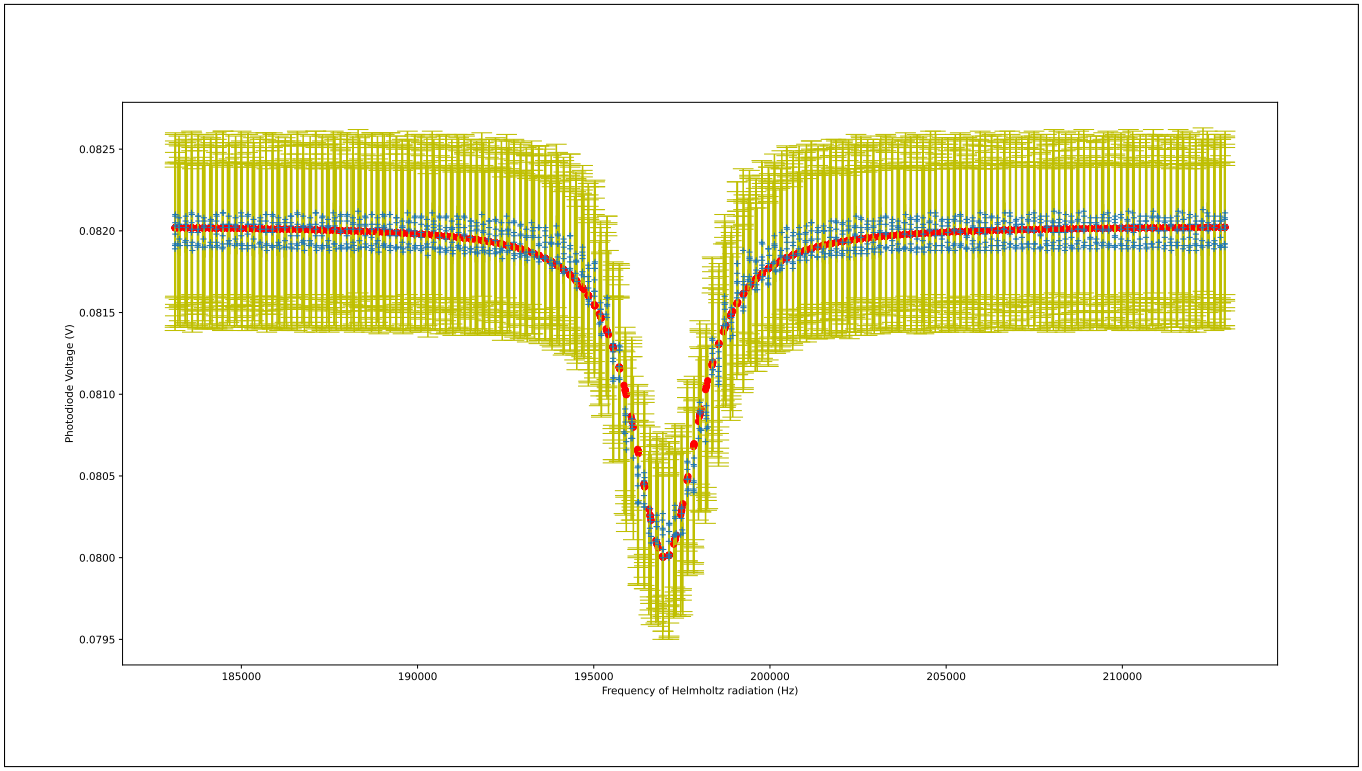

Figure 5. ^{85}Rb Lorentzian Zeeman peak at ambient magnetic field

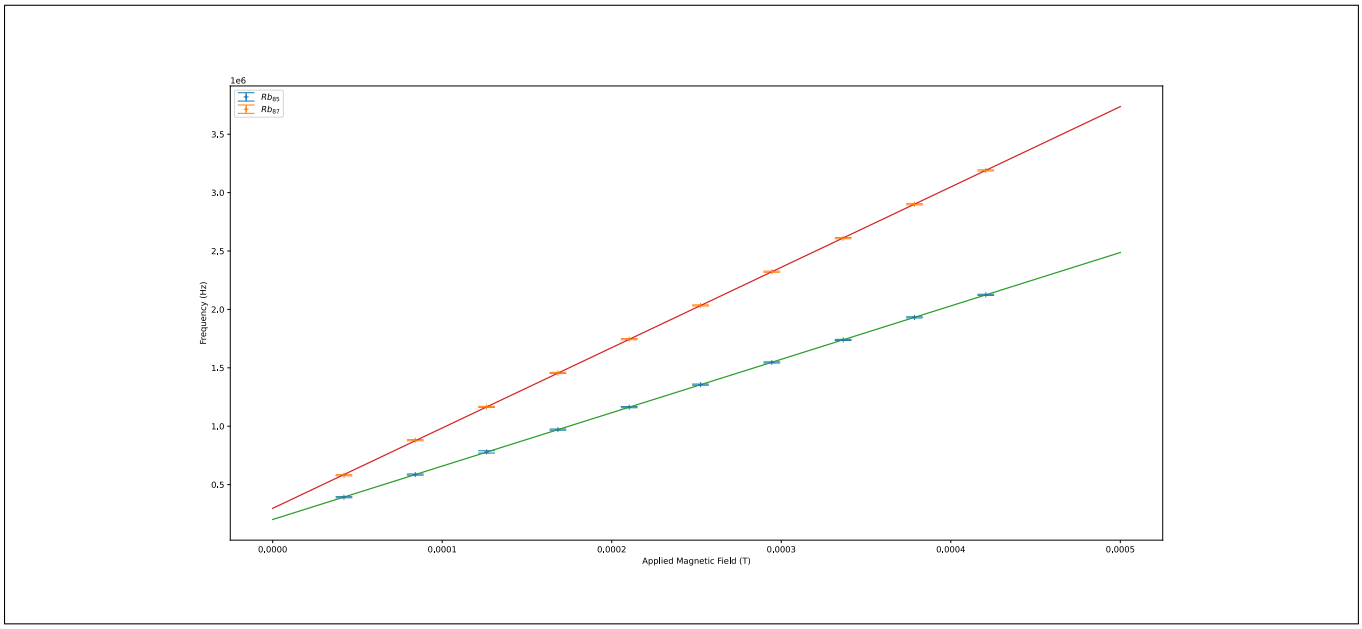

Figure 6. Frequency of dip vs applied magnetic field

is that the coupling between the spin angular momentum and the orbital angular momentum is lost (ie. they can no longer be treated as averaging out to a single J vector precessing about the magnetic field vector.)

In the case where $j = 1/2$, the energy shift of magnetic sub levels of the ground state can be described in closed form by the Breit-Rabi Formula (Equation 6). A plot of the shift as a function of the applied magnetic field is shown in Figure 7.

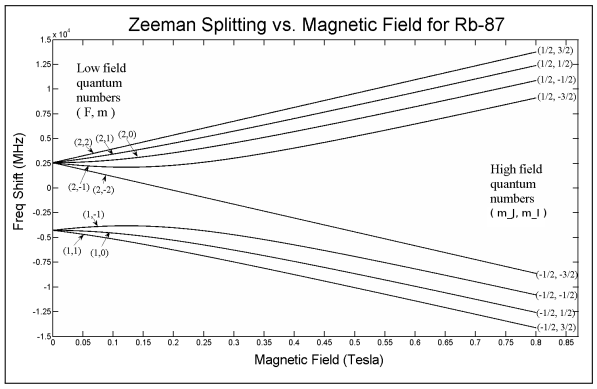

Figure 7. Reproduced here under the terms of the CC-BY-SA license (attrib user Danski14 on Wikipedia)

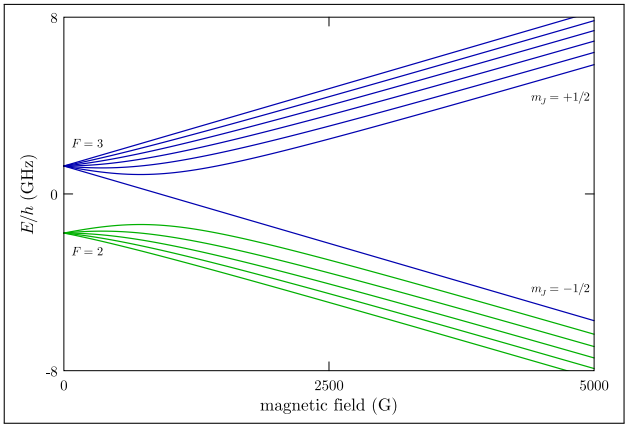

Figure 8. $^{85}Rb\,5^2S_{1/2}$ level hyperfine structure in external field (From [13])

$$\Delta E_{F=I\pm1/2} = -\frac{h\Delta W}{2(2I+1)} + \mu_{\mathrm{N}} g_I m_F B \pm \frac{h\Delta W}{2}\sqrt{1+\frac{2m_F x}{I+1/2}+x^2}$$

$$x \equiv \frac{B(\mu_{\mathrm{B}} g_J - \mu_{\mathrm{N}} g_I)}{h\Delta W} \qquad \Delta W = A\left(I+\frac{1}{2}\right) \quad \text{where } \Delta W \text{ is the zero-field splitting} \tag{6}$$

From Equation 6, it is clear that the only nonlinear factor in $m_f$is $\frac{h\Delta W}{2}\sqrt{1+\frac{2m_F x}{I+1/2}+x^2}$. Clearly the energy differences reduce with increase $m_f$number for $F = I + 1/2$. Also, from Figure 9 it is apparent that the pumped state is the one with the lowest adjacent transition energy. Therefore, the light entering the cell is σ^+ polarized.

D. Observation of Multiphoton Transitions in ^{87}Rb

At very high amplification and high magnetic field, the RF coils can induce increased absorption at the photodiode at the arithmetic mean of two resonant frequencies. This could be because of *multiphoton absorptions*, ie. instead of a transition from $5^2S_{1/2}M_F = 2$ to $5^2S_{1/2}M_F = 1$ due to an $E = hf_1$ resonance or $5^2S_{1/2}M_F = 1$ to $5^2S_{1/2}M_F = 0$due to an $E = hf_2$resonance; there is a $5^2S_{1/2}M_F = 2$ to $5^2S_{1/2}M_F = 0$ transition due to an $E = 2hf_3$ resonance, where $f_3 = \frac{f_1+f_2}{2}$. Two possible candidates for multiphoton transition peaks are recorded in Figure 10.

III. CONCLUSION

As demonstrated, the technique of optical pumping can be used to make measurements of low energy phenomena such as the Zeeman Effect. In this demonstration, these measurements are used to infer remarkably accurate values for the hyperfine Landé g-factor and Earth's magnetic field at Stony Brook. It is also, of course, a very interesting phenomenon in and of itself.

I develop a qualitative foundation for understanding Optical Pumping and the Zeeman Effect experiment. I also present evidence for the existence of multiphoton absorption in optically pumped^{87}Rb by showing overlaid oscilloscope traces with RF intensity dependent peaks at the arithmetic mean of subsequent resonant frequencies.

Further work is needed to see if the proposed thermodynamic mechanism for peak heights mentioned in Section I C is valid. Since it predicts that the relative height difference between peaks should increase dramatically at lower temperatures, a relatively easy test would be to perform the experiment with the rubidium cell immersed in liquid nitrogen.

More work is also needed to determine the exact mechanism for multiphoton resonances. While the phenomenon observed certainly resembles two photon absorption, it may have an entirely innocuous classical electrodynamics explanation. If it really *is* multi photon absorption, then this experiment would be a way of observing this effect without a laser, which would be pretty cool.

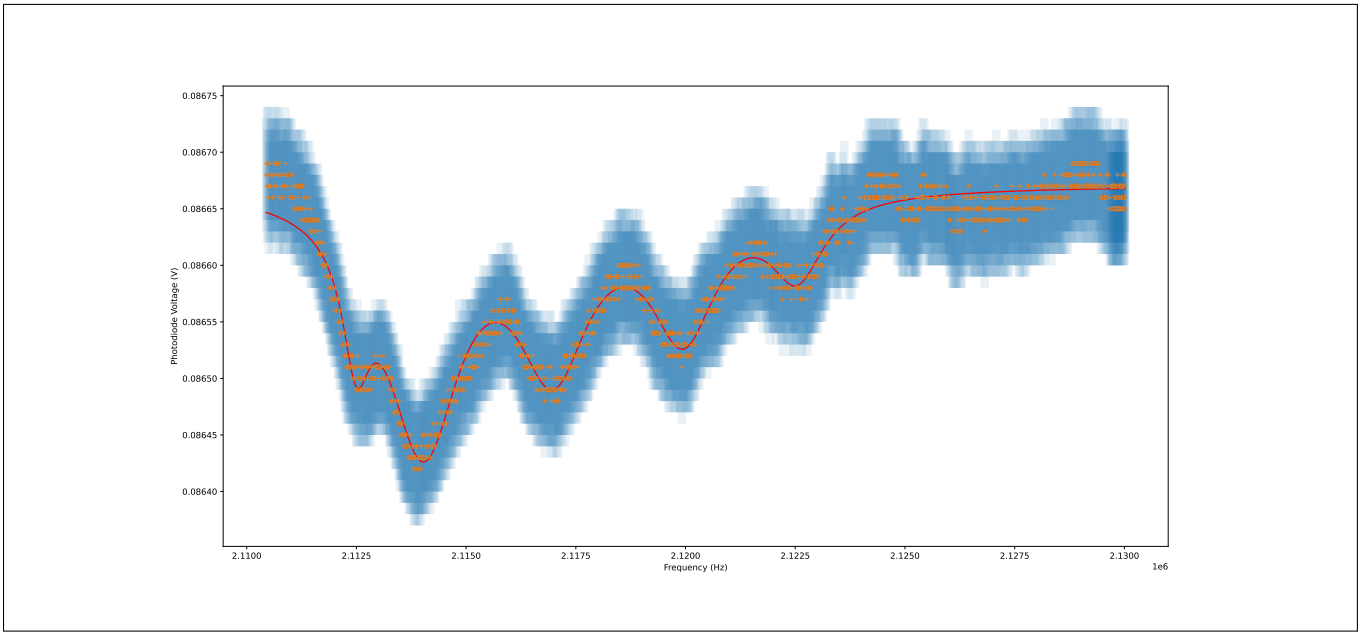

Figure 9. Oscilloscope trace with 1A Current in Helmholtz Coils ($420\,\mu T$) and Function Generator Sweeping from 2.11 Mhz to 2.13 Mhz. Fit is a sum of five lorentzian distributions.

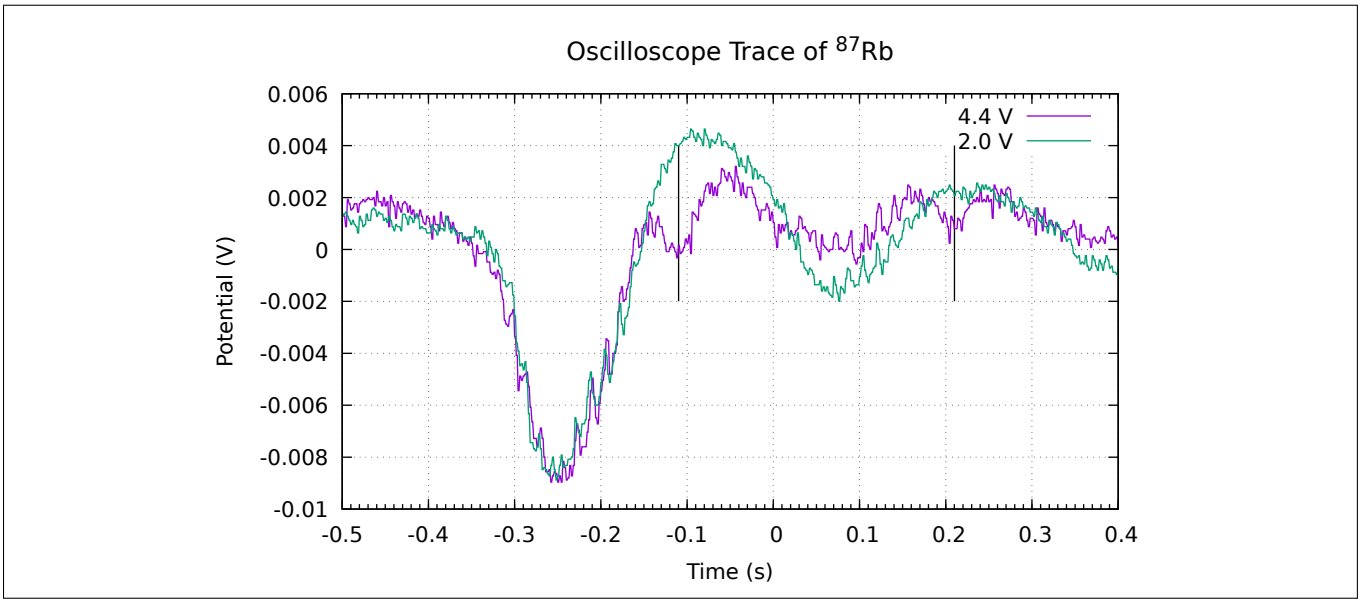

Figure 10. Oscilloscope trace with 1.5A Current in Helmholtz Coils ($630\,\mu T$) and Function Generator Sweeping from 4.615 Mhz to 4.635 Mhz with Amplitudes of 4.4V and 2.0V (black lines indicate multiphoton peaks.)

ACKNOWLEDGMENTS

I thank Professor Figueroa for all his help with this experiment, as well as TA Shane Andrewski for supervising me in the lab after hours and also helping tremendously with debugging the experimental setup.

Special thanks to my lab partner, Joseph Monroy, for performing the experiments with me.

[1] Quantum Physics, 3rd Edition | Wiley, . URL https://www.wiley.com/en-us/Quantum+Physics%2C+3rd+Edition-p-9780471057000.

[2] tikz pgf - Energy level diagrams with TeX, . URL

https://tex.stackexchange.com/questions/124269/energy-level-diagrams-with-tex.

[3] Stony Brook Physics Dept . PHY 445/515 Optical Pumping and Magnetic Resonance, 2021.

[4] National Geophysical Data Center. NCEI Geomagnetic Calculators. URL https://www.ngdc.noaa.gov/geomag/calculators/magcalc.shtml#igrfwmm. Publisher: U.S. Department of Commerce.

[5] Abhishek Cherath and Joseph Monroy. Optical Lab. URL https://deepnote.com/project/Optical-Lab-70JaJlJhQL2FdiWaBAeOJg/%2Fearth_field.ipynb.

[6] Abhishek Cherath and Joseph Monroy. Optical Pumping Lab Report, August 2021.

[7] Adam Egbert, Will Wiegand, and Hannah Sheppard. Optical Pumping of Rubidium. page 4.

[8] Jonathon Garamella. Optical Pumping of Rubidium. page 4.

[9] Note1. *In the following discussion, we assume* $\sigma = 1$ *without loss of generality.*

[10] Note2. The measured x, R values can be checked in the referred python notebook[5].

[11] Penhurst Park. A PRODUCT OF TEACHSPIN, INC. page 94.

[12] D. Steck. Rubidium 87 D Line Data. *undefined*, 2003. URL https://www.semanticscholar.org/paper/Rubidium-87-D-Line-Data-Steck/c189dd12981e1d94ac53fdae4f0f804cc297503b.

[13] DA Steck. Rubidium 85 D line data. URL https://steck.us/alkalidata/rubidium85numbers.pdf.